Reversible cytoplasmic localization of the proteasome in quiescent yeast cells

Damien Laporte,[1,2] Bénédicte Salin,[1,2] Bertrand Daignan-Fornier,[1,2] and Isabelle Sagot[1,2]

[1]Institut de Biochimie et Génétique Cellulaires, Université Victor Segalen Bordeaux II, 33077 Bordeaux, France
[2]Centre National de la Recherche Scientifique, UMR5095 Bordeaux, France

The 26S proteasome is responsible for the controlled proteolysis of a vast number of proteins, including crucial cell cycle regulators. Accordingly, in *Saccharomyces cerevisiae*, 26S proteasome function is mandatory for cell cycle progression. In budding yeast, the 26S proteasome is assembled in the nucleus, where it is localized throughout the cell cycle. We report that upon cell entry into quiescence, proteasome subunits massively relocalize from the nucleus into motile cytoplasmic structures. We further demonstrate that these structures are proteasome cytoplasmic reservoirs that are rapidly mobilized upon exit from quiescence. Therefore, we have named these previously unknown structures proteasome storage granules (PSGs). Finally, we observe conserved formation and mobilization of these PSGs in the evolutionary distant yeast *Schizosaccharomyces pombe*. This conservation implies a broad significance for these proteasome reserves.

Introduction

In actively proliferating budding yeast, proteasome 26S is the most abundant cellular form of the proteasome holoenzyme (Bajorek et al., 2003). It consists of a 20S core particle (CP), containing α and β subunits arranged into a barrel-shaped complex that bears the proteolytic activity and a 19S regulatory particle (RP) made up of two subcomplexes: the base and the lid (Hanna and Finley, 2007). However, the 26S holoenzyme is not the sole proteasome form and subcomplexes can be found associated with other regulatory partners (Schmidt et al., 2005).

The proteasome 26S degrades polyubiquitylated substrates in an ATP-dependent fashion (Hanna and Finley, 2007). It can also degrade specific nonubiquitylated target proteins (Orlowski and Wilk, 2003). In budding yeast, the majority of long-lived proteins are not degraded by the proteasome, whereas short-lived protein degradation is strongly affected by proteasome inhibitors (Lee and Goldberg, 1996). Many of the short-lived targets of the proteasome are proteins involved in cell cycle progression. Consequently, a functional proteasome is crucial for cell proliferation. Accordingly, in budding yeast, all but four proteasome subunits are encoded by essential genes. Besides, proteolysis is not the sole function of proteasome subcomplexes, and it has been established that the 19S RP plays an important role in transcription regulation (Ferdous et al., 2001; Collins and Tansey, 2006; Sulahian et al., 2006).

In exponentially growing yeast cells, 80% of the 26S proteasome is localized inside the nucleus throughout the cell cycle (Russell et al., 1999). In *Schizosaccharomyces pombe*, the nuclear envelope protein Cut8 is required for the retention of the proteasome 26S inside the nucleus (Tatebe and Yanagida, 2000; Takeda and Yanagida, 2005). It is widely accepted that precursors of both the 20S and 19S particles are translocated independently into the nucleus via the karyopherin αβ pathway, where they are subsequently maturated and assembled into active 26S holoenzymes (Lehmann et al., 2002; Fehlker et al., 2003; Heinemeyer et al., 2004; Wendler et al., 2004; Isono et al., 2007; Li et al., 2007).

Surprisingly, little is known about the proteasome in nonproliferating cells. It has been shown that the proteasome proteolytic activity decreases upon cells' entry into stationary phase (Bajorek et al., 2003). This effect, apparently, does not correlate with a decrease of proteasome subunit abundance (Fig. S1, available at http://www.jcb.org/cgi/content/full/jcb.200711154/DC1; Bajorek et al., 2003) but rather with a disassembly of 19S RP from the 26S holoenzyme. Upon exit from quiescence, cells rapidly reassemble 26S proteasomes (Bajorek et al., 2003). Although the expression of a constitutively active mutant form of the 20S CP decreases long-term cell survival, the cellular role of the proteasome and the fate of disassembled subcomplexes in quiescent cells remain obscure.

Correspondence to Isabelle Sagot: isabelle.sagot@ibgc.u-bordeaux2.fr

Abbreviations used in this paper: CP, core particle; PSG, proteasome storage granule; RP, regulatory particle.

The online version of this paper contains supplemental material.

The Rockefeller University Press $30.00
J. Cell Biol. Vol. 181 No. 5 737–745
www.jcb.org/cgi/doi/10.1083/jcb.200711154

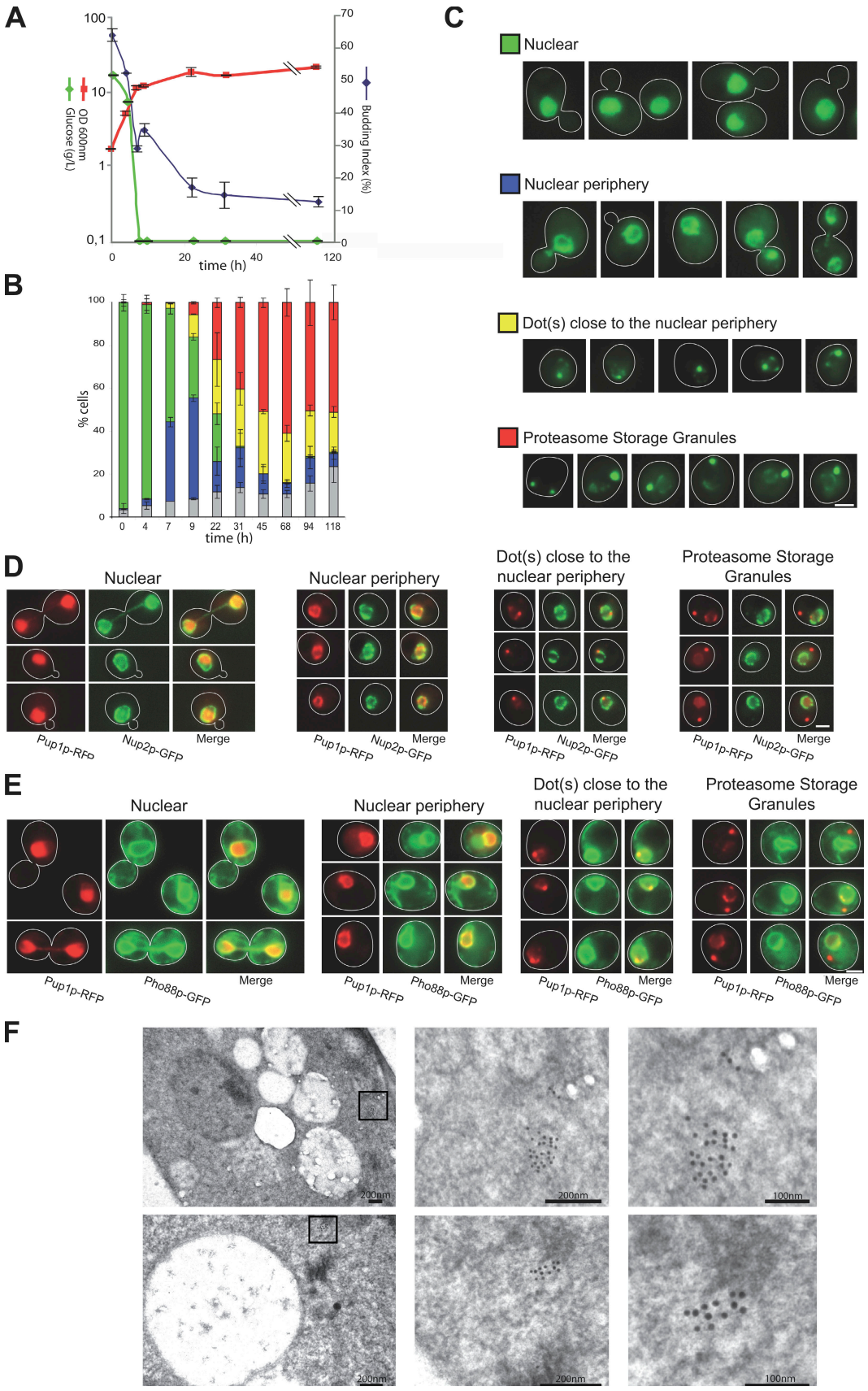

Figure 1. **Proteasome relocalization upon entry into quiescence.** (A–C) Cells expressing Pre6p-GFP were grown in YPDA medium at 30°C. (A) At various stages of growth, OD 600 nm was monitored (red curve), glucose concentration in the medium was measured (green curve), and the budding index was determined (blue curve; $n > 200$ cells for each time point). (B) Localization of Pre6p-GFP. For each time point, the localization of Pre6p-GFP fluorescence

In this paper, we show that upon *Saccharomyces cerevisiae* entry into quiescence, there is a massive cytoplasmic relocalization of proteasome subunits into new structures that we have named proteasome storage granules (PSGs). This phenomenon is rapidly and fully reversed upon cell reentry into the proliferation cycle. Importantly, nuclear relocalization upon exit from quiescence occurs even in the absence of de novo protein synthesis, implying that PSGs are storage structures. Both PSG formation and nuclear relocalization were observed in the evolutionary distant yeast *S. pombe*, demonstrating the strong conservation and the broad significance of this phenomenon.

Results and discussion

Proteasome relocalization upon entry into quiescence

We first followed the localization of Pre6p, an α 20S CP subunit, in living yeast cells. When fused to GFP at its C terminus, Pre6p can properly be incorporated into active 26S proteasomes (Enenkel et al., 1998) and, accordingly, a strain expressing Pre6p-GFP as a sole source of Pre6p did not show any growth defect (unpublished data). As previously shown by others (Enenkel et al., 1998; Lehmann et al., 2002; Isono et al., 2007), Pre6p-GFP was localized in the nucleus of actively proliferating cells (Fig. 1, A–C, green bars [B]). This was verified in a strain coexpressing the 20S CP subunit Pup1p fused to RFP together with either the nuclear pore complex protein Nup2p fused to GFP (Fig. 1 D, left) or the endoplasmic reticulum membrane protein Pho88p fused to GFP (Fig. 1 E, left). Of note, the proteasome was clearly excluded from the nucleolus. Surprisingly, upon glucose exhaustion, Pre6p-GFP relocalized to the nuclear periphery (Fig. 1, A–C, blue bars [B]). The colocalization with Nup2p-GFP and Pho88p-GFP (Fig. 1, D and E, respectively, middle left) attested that the proteasome indeed relocalized very close to or at the nuclear membrane. It should be noted that chemical fixation or cell wall stresses caused a similar relocalization of Pre6p-GFP from the nucleus to the nuclear periphery in exponentially growing cells (unpublished data). This observation could explain contradictions in earlier reports regarding proteasome localization in actively dividing yeast cells, which was either described as nucleoplasmic (McDonald and Byers, 1997; Russell et al., 1999; Wendler et al., 2004; Isono et al., 2007) or associated with the nuclear envelope (Enenkel et al., 1998).

Strikingly, when cells stopped to proliferate and entered quiescence upon carbon source exhaustion (early stationary phase), Pre6p-GFP adopted an original and complex localization. Indeed, most of the Pre6p-GFP fluorescence was detected as bright dots that could either be localized close to the nuclear periphery and immobile (minor population; Fig. 1, A–C, yellow bars [B]; and Fig. 1 D and E, colocalization experiments) or freely mobile within the cytoplasm (majority of the cells; Fig. 1, A–C, red bars [B]). As shown in Fig. 1 C, one or two bright dots of variable size were observed per cell. In addition, a faint Pre6p-GFP signal could be detected at the nuclear periphery in most of the cells (Fig. 1, C–E). The typical relocalization into cytoplasmic dot was observed for nine other 20S CP subunits and eleven 19S RP subunits (Table S1, available at http://www.jcb.org/cgi/content/full/jcb.200711154/DC1). Importantly, proteasome cytoplasmic dots could also be detected by electron microscopy in wild-type quiescent cells using antibodies against 20S CP subunits and gold particle–labeled secondary antibodies (Fig. 1 F). The cytoplasmic clusters of gold particles were not associated with specific organelles or any detectable membrane. From those experiments, we conclude that in quiescent cells, all the proteasome subunits that we have tested massively localize into cytoplasmic dots. We named these structures PSGs.

19S and 20S subunits relocalize simultaneously into PSGs

Although all tested proteasome subunits relocalized as cytoplasmic dots in yeast quiescent cells, we asked whether subunits from the various subcomplexes colocalize within the same dots. Data shown in Fig. 2 A clearly established that subunits of the 20S CP and 19S RP colocalized within the same PSG in cells grown 4 d. Furthermore, upon culture aging, whatever the stage of growth, Scl1p-GFP (20S CP, α subunit) was always colocalized with Pup1p-RFP (20S CP, β subunit; Fig. 2 B). The same observations were made for Sem1p-GFP (19S RP, lid) and Pup1p-RFP (20S CP, β subunit; unpublished data). Consequently, different proteasome subunits simultaneously relocalized into PSGs upon cell entry into quiescence.

In quiescent yeast cells, although it has been shown that the 26S proteasome is disassembled in crude extracts, we clearly demonstrate here that in vivo most of the 19S and 20S subunits are colocalized in PSGs. Thus, our results imply that differential localization of the proteasome subunits cannot account for the reported reduction of proteasome activity in quiescent cell extracts. In addition, it was established that mature 20S CP subcomplexes remained assembled throughout stationary phase (Bajorek et al., 2003); therefore, it is likely that PSGs contain assembled 20S CPs that have relocalized after maturation inside the nucleus. Native gel electrophoresis confirmed that after 4 d,

was scored as nuclear (green bar), at the nuclear periphery (blue bar), immobile dots close to the nuclear periphery (yellow bar), or bright mobile cytoplasmic dots (PSG) with or without nuclear periphery staining (red bar; $n > 200$ cells for each time point; two experiments; error bars show SD). The gray bars represent the percentage of cells in which GFP fluorescence was not detectable. (C) Typical images of each Pre6p-GFP localization patterns are shown. Images are maximal projection of 0.2-µm z stacks. Of note, for localization of Pre6p-GFP at the nuclear periphery, images were taken with an exposure time that was three times longer than for the other images. Furthermore, levels of gray of the top two rows of images range from 0 to 800 and the levels of gray of the two bottom rows of images range from 0 to 3,000. (D) Colocalization of the proteasome (as revealed by the 20S CP subunit Pup1p fused to RFP) and the nuclear envelope (as revealed by the nuclear pore complex protein Nup2p fused to GFP). (E) Colocalization of the proteasome (as revealed by the 20S CP subunit Pup1p fused to RFP) and the endoplasmic reticulum (as revealed by the membrane protein Pho88p fused to GFP). Images in D and E are single focal planes. Bars, 2 µm. (F) Immunolocalization using anti-20S CP antibodies detected with secondary antibodies linked to 10-nm gold particles in wild-type yeast cells grown for 4 d at 30°C in YPDA medium.

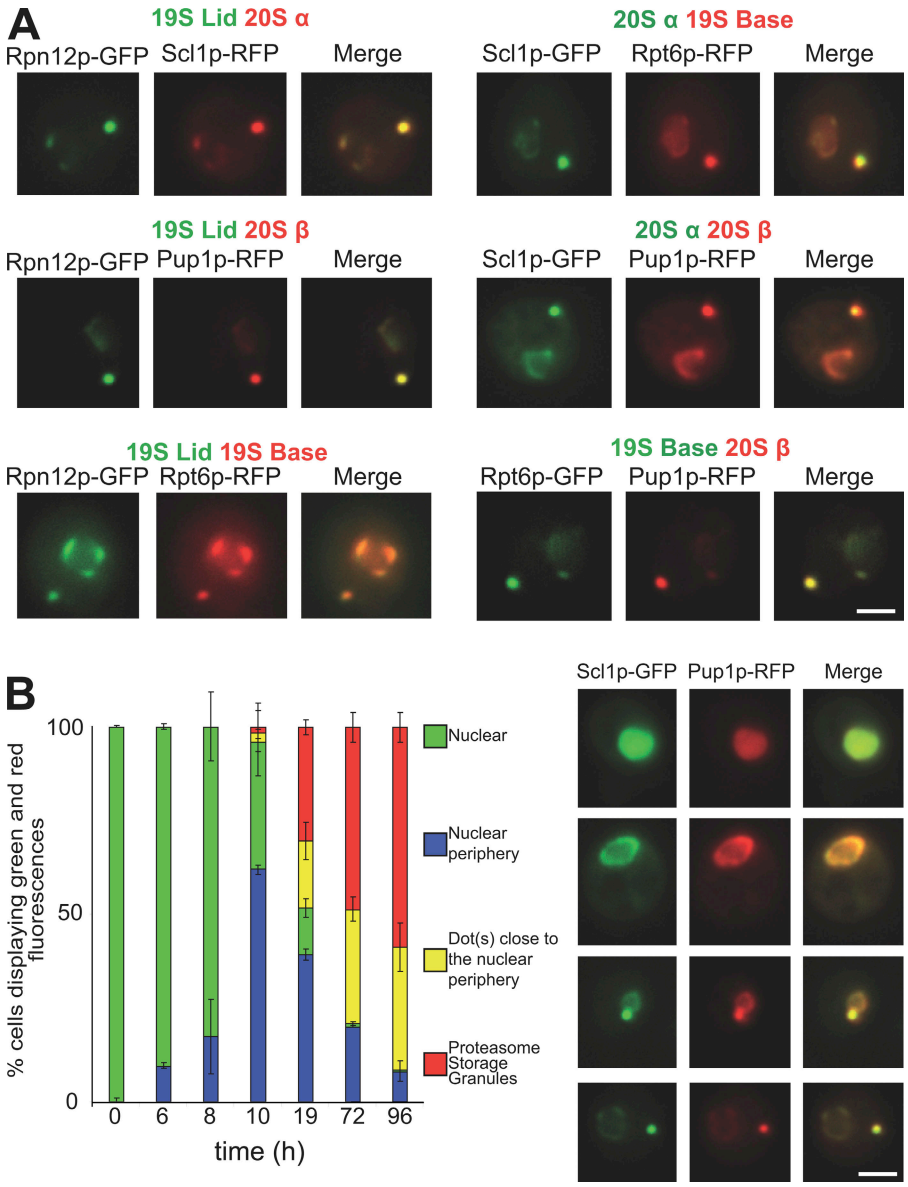

Figure 2. **19S and 20S proteasome subunits colocalization.** (A) Colocalization of 19S RP and 20S CP proteasome subunits in quiescent yeast cells. Cells coexpressing the indicated fusion proteins were imaged after 4 d of growth in YPDA at 30°C. GFP fluorescence is green and RFP fluorescence is red. Images are single focal planes. (B) Cells expressing Scl1p-GFP and Pup1p-RFP were grown in YPDA medium at 30°C. For each time point, cells displaying both the green and the red fluorescence were scored as indicated in the Fig. 1 legend. For each time point, $n > 200$ (two experiments; error bars show SD). Typical colocalization images corresponding to each type of proteasome localization pattern are shown on the right. Images are maximal projection of z stacks. Bars, 2 µm.

the 20S CP remained assembled. However, in our hands, assembled 26S was still detectable in quiescent cells (Fig. S2. available at http://www.jcb.org/cgi/content/full/jcb.200711154/DC1). This discrepancy with Bajorek et al. (2003) remains to be clarified. Besides, whether 20S CPs in PSGs are associated with 19S RP subunits and/or other partners waits for the purification of intact PSGs. All our attempts to address the proteolytic activity of the proteasome embedded into PSGs in living quiescent cells have failed. Therefore, whether the proteasome subunits in PSGs are assembled into active complexes remains an open question.

PSGs do not colocalize with other quiescent cell structures

In our growth conditions, entry into quiescence is a consequence of glucose exhaustion, yet PSG formation could also be observed in cells grown on respiratory carbon sources (Fig. 3 A) and, as such, do not constitute a specific response to glucose deprivation. Instead, our data indicate that PSGs are structures typical of nonproliferating cells. Of note, PSGs were also observed in quiescent diploid cells (Fig. 3 A). Recently, we have described actin structures that appear in yeast quiescent cells: the actin bodies (Sagot et al., 2006). As shown in Fig. 3 B, PSGs and actin bodies did not colocalize in quiescent cells. Similarly, the formation of P-bodies, a structure containing RNA and RNA-modifying proteins, is also triggered upon entry into quiescence (Parker and Sheth, 2007). As shown in Fig. 3 C, Dcp2p-GFP, a specific marker of P-bodies, did not colocalize with PSGs. Thus, actin bodies, P-bodies, and PSGs are distinct cytoplasmic structures.

Because PSGs are detected a few hours after carbon source exhaustion, their formation could either be a passive consequence of the general cell metabolism slowing down upon entry into quiescence or could be actively triggered by a not yet defined molecular process. PSGs and actin bodies appear with similar kinetics, suggesting that the formation of these structures could possibly rely on interconnected signaling cascades.

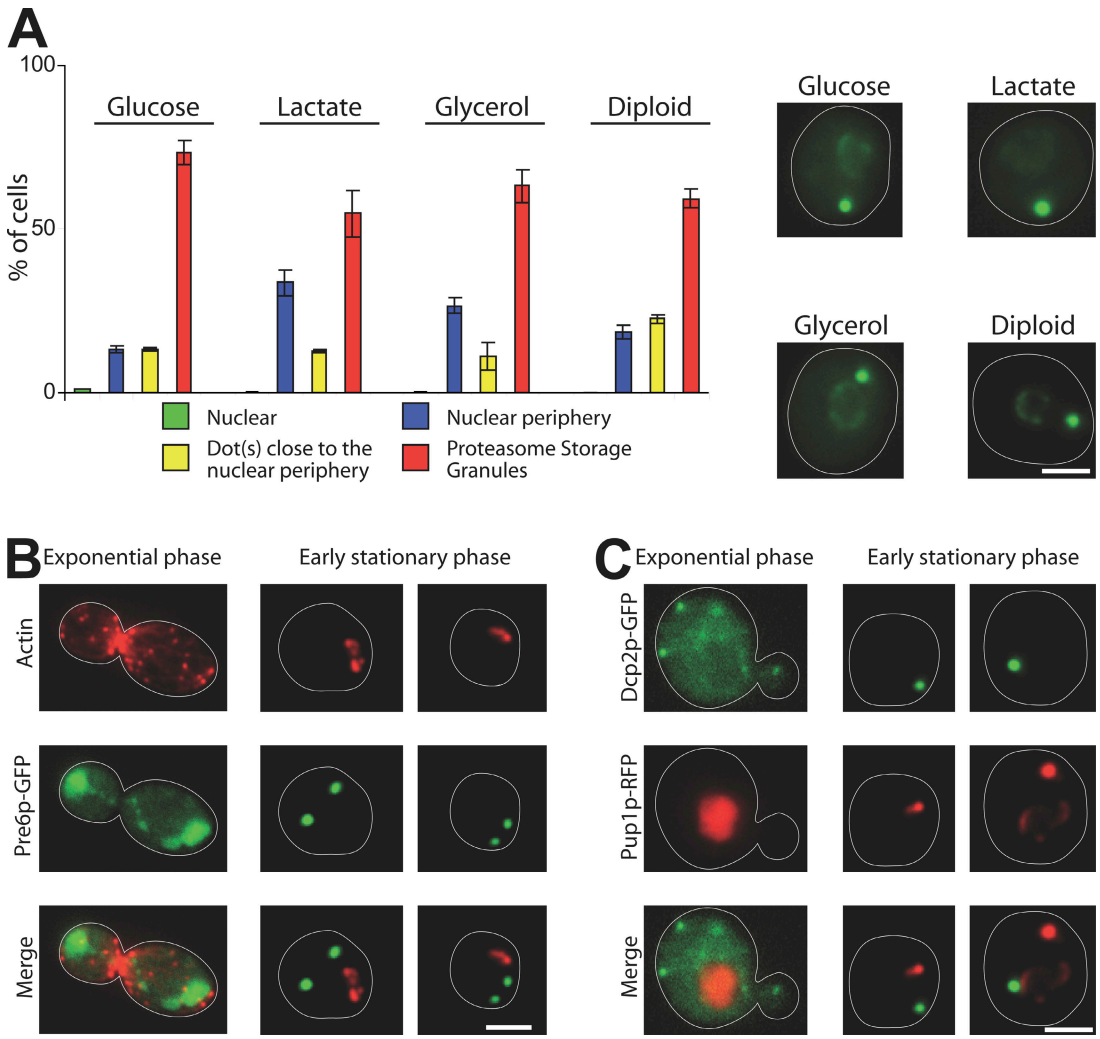

Figure 3. **PSGs, actin bodies, and P-bodies are distinct structures.** (A) PSGs, as revealed by Pre6p-GFP fluorescence, were observed in cells grown for 4 d in different carbon sources containing rich media and in diploid cells grown in YPDA. For each condition $n > 200$ (two experiments; error bars show SD). Typical images (maximal projection of z stacks) of cells displaying PSGs (Pre6p-GFP) are shown on the right. (B) Cells expressing Pre6p-GFP were grown in YPDA medium at 30°C, fixed, and stained with Alexa Fluor phalloidin to reveal F-actin–containing structures. Actively proliferating cells (left) displayed actin patches and cables (red) and a typical Pre6p-GFP nuclear localization. Quiescent cells displayed PSGs (green fluorescence) that did not colocalize with actin bodies (red). (C) Cells coexpressing Dcp2p-GFP and Pup1p-RFP were grown in YPDA medium at 30°C. Actively proliferating yeast cells displayed a typical Pup1p-RFP nuclear localization and small and discrete Dcp2p-GFP dots. In quiescent cells, Dcp2p-GFP localized in P-bodies that did not colocalize with PSGs. Images in B and C are single focal planes. Bars, 2 µm.

Importantly, the discovery of PSGs strongly supports the idea of a massive reorganization of cellular structures upon entry into quiescence.

PSGs: rapidly available proteasome reserves?

In contrast to actin bodies, we observed that PSGs were highly mobile within the cytoplasm. This is in agreement with the fact that the cytoplasmic clusters of gold particles detected by electron microscopy were not associated with specific organelles (Fig. 1 F). We measured PSG mobility and observed that the speed of a PSG decreased with the age of the quiescent cells. Indeed, in cells expressing Scl1p-GFP, the mean speed decreased from 83 ± 58 nms^{-1} (n = 1,199 displacements) after 3 d to 18 ± 16 nms^{-1} after 7 d of growth (n = 840 displacements; Fig. S3 A, available at http://www.jcb.org/cgi/content/full/jcb.200711154/DC1). Similar results were obtained for Pup1p-RFP (unpublished data). In parallel, we measured the evolution of PSG fluorescence intensity. The mean fluorescence intensity of Scl1p-GFP increased by approximately twofold between days 3 and 7 of culture (Fig. S3 B; similar results were obtained for Pup1p-RFP [unpublished data]). These data strongly suggest that there is a time-dependent accumulation of proteasome subunits within PSGs.

All our previous data point at PSGs as proteasome storage structures. If this is the case, proteasome subunits embedded into PSGs should be mobilized upon cell exit from quiescence. Wild-type cells expressing Pre6p-GFP were grown for 4 d in YPD medium and then either transferred into water or refed with new YPD medium. Although no change in Pre6p-GFP localization was detected when cells were transferred to water (Fig. 4 A), a very fast and drastic relocalization of Pre6p-GFP was observed upon

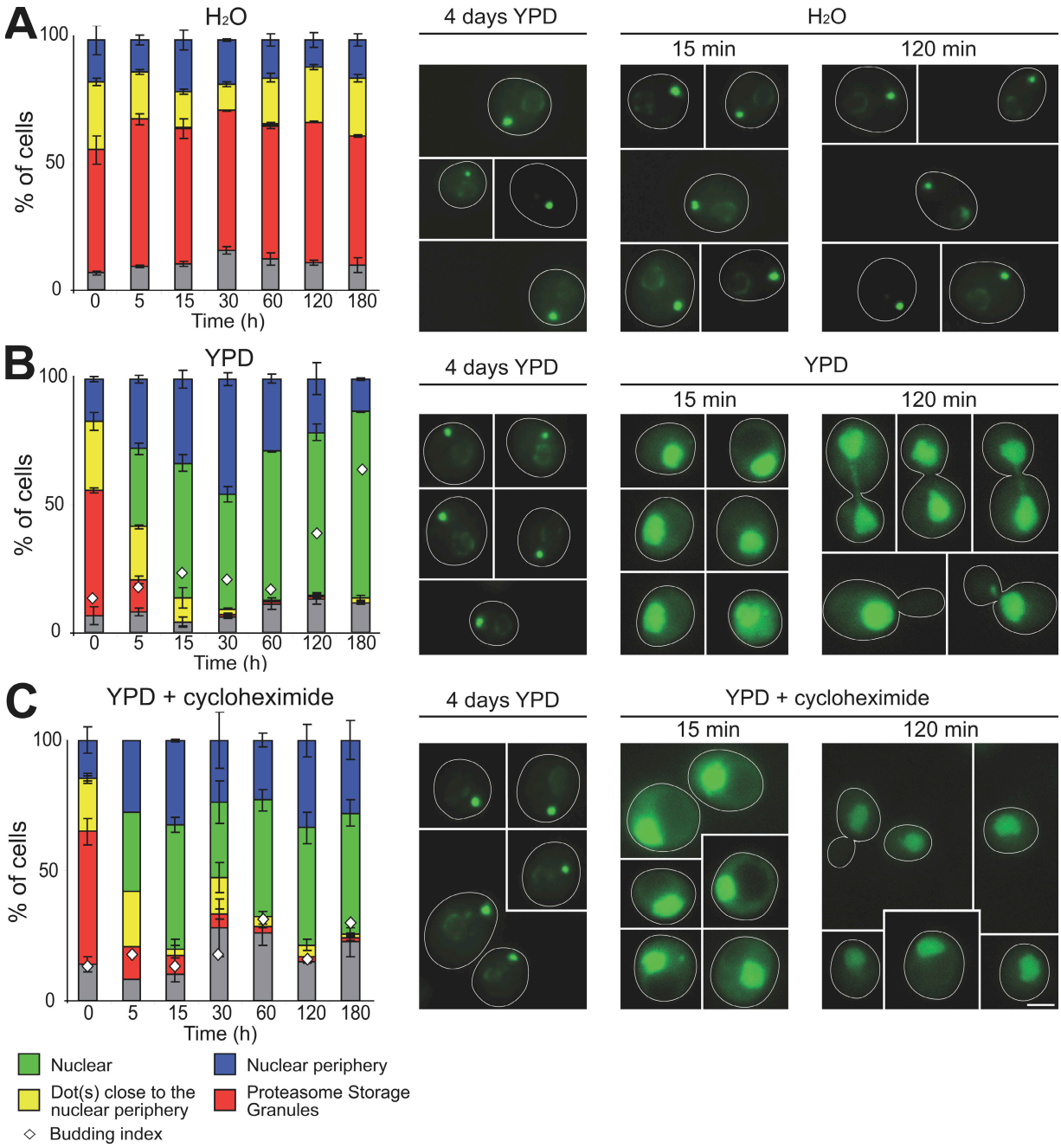

Figure 4. **PSGs are rapidly mobilized upon exit from quiescence.** Cells expressing Pre6p-GFP were grown for 4 d in YPD medium at 30°C, washed, and either resuspended in water (A) or new YPD medium (B) or preincubated for 1 h in old YPD medium containing 100 µg/ml cycloheximide and then released into new YPD medium containing 100 µg/ml cycloheximide (C). For each time point, cells displaying Pre6p-GFP fluorescence within PSGs, immobile dots close to the nuclear periphery, nuclear periphery, or nucleus were counted ($n > 200$; two experiments; error bars show SD). The budding index is indicated ($n > 200$; two experiments; SD < 5%). Images are maximal projection of z stacks. Bar, 2 µm. Of note, the levels of gray for images where PSGs are detected range from 0 to 1,500, and they range from 0 to 500 for images where the fluorescence is detected at the nuclear periphery or in the nucleus.

cell refeeding (Fig. 4 B). Indeed, within <15 min after transfer of the cells to new YPD medium, all the Pre6p-GFP fluorescence was detected within the cell nuclei (first at the nuclear periphery and then into the nucleus). Importantly, the mobilization of Pre6p-GFP upon cell exit from quiescence could occur in the absence of de novo protein synthesis because cycloheximide did not prevent the relocalization of Pre6p-GFP to the nucleus (Fig. 4 C). The same results were obtained with Scl1p-GFP, Rpt6-GFP, and Rpn11-GFP (unpublished data). Therefore, PSGs contain available proteasome subunits that can be rapidly mobilized and, as such, could be defined as proteasome cytoplasmic reserves.

Why would quiescent cells store proteasome in PSGs instead of degrading 20S CPs and their regulatory components? It could be that upon exit from quiescence, cells need to rapidly and massively degrade proteins such as those damaged during quiescence. Proteasome subunits, like actin, are abundant proteins (~1% of the total yeast proteins; Russell et al., 1999) and both are stored in structures that are rapidly mobilized

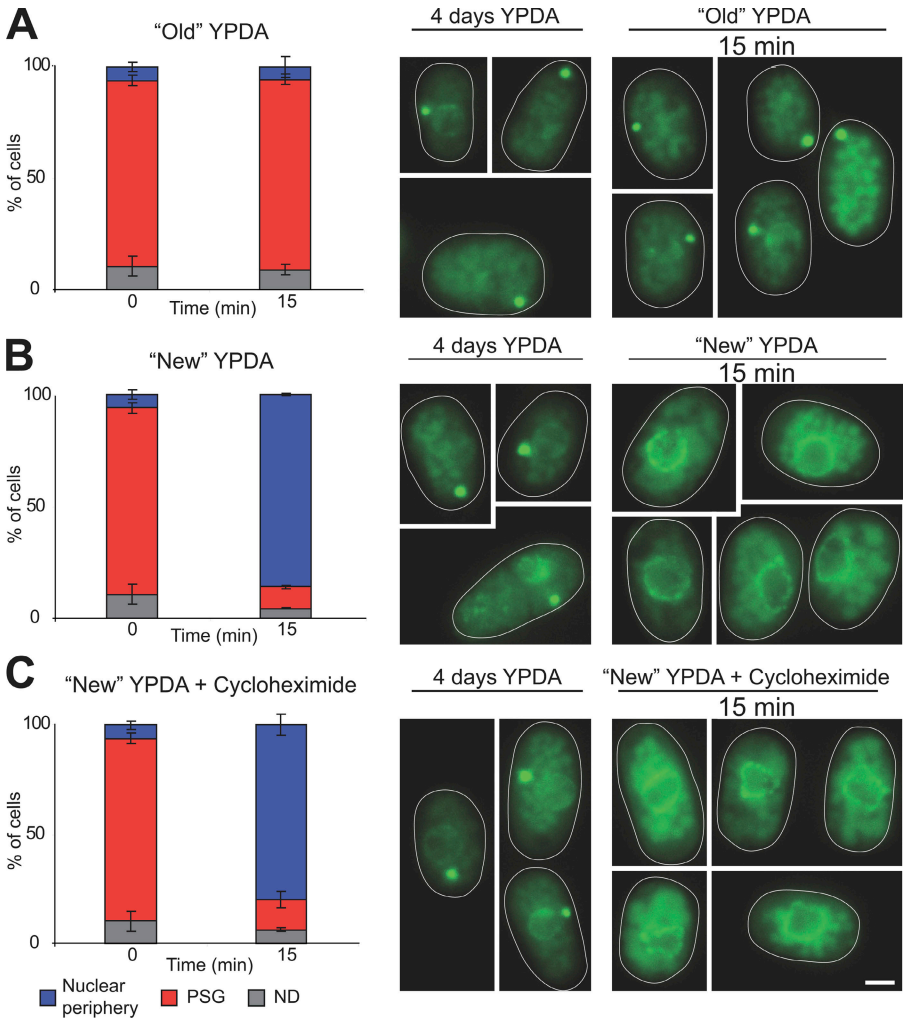

Figure 5. ***S. pombe* cells display PSG.** *S. pombe* expressing Pad1-GFP (Rpn11 homologue) were grown for 4 d in YPDA medium at 30°C, washed, and resuspended either in water (A) or new YPDA medium (B) or preincubated for 1 h in old YPDA medium containing 100 µg/ml cycloheximide and then released into new YPDA medium containing 100 µg/ml cycloheximide (C). For each time point, cells displaying Pad1-GFP fluorescence within PSG or at the nuclear periphery were counted (n > 200; two experiments; error bars show SD). Images are maximal projection of z stacks. Bar, 2 µm. Of note, cycloheximide was active on *S. pombe* cells because 2 h after refeeding in the presence of the drug, cells did not grow and displayed a round-shape morphology, whereas the untreated cells elongated and started to divide. The mean cell size before exit from quiescence was 7.44 ± 0.86 µm (n = 50). 3 h after transfer of quiescent cells to new YPDA medium, mean cell size increased (13 ± 2 µm; n = 50). In contrast, 3 h after transfer of quiescent cells to new YPDA medium containing 100 µg/ml cycloheximide the cell size did not significantly change (8.35 ± 1.16 µm; n = 50).

upon exit from quiescence (Sagot et al., 2006; this work). If proteasome subunits were degraded in quiescent cells, replenishing the pool of proteasome subunits upon exit from quiescence might cause a delay for cell reentry into the proliferation cycle and as such would reduce fitness. Finally, we cannot rule out the possibility that in quiescent cells, the proteasome subunits embedded into PSGs have other activities that are or are not related to protein degradation. Future studies based on mutants should help to decipher PSGs' precise cellular function.

S. pombe quiescent cells display PSGs

In actively proliferating *S. pombe*, Pad1, the Rpn11p homologue, is localized within the nucleus (Wilkinson et al., 1998; unpublished data). Similar to *S. cerevisiae*, in *S. pombe*, after 4 d of growth, we detected Pad1-GFP fluorescence as a motile cytoplasmic dot (Fig. 5). Furthermore, upon exit from quiescence, Pad1-GFP rapidly relocalized from this cytoplasmic structure to the nuclear periphery (Fig. 5 B) and, later, to the nucleus (not depicted). As this relocalization could occur in the absence of de novo protein synthesis (Fig. 5 C), we can conclude that in quiescent *S. pombe* cells, just as in *S. cerevisiae*, the proteasome accumulates as a cytoplasmic reserve that can rapidly be mobilized upon cell reentry into the proliferation cycle.

In mammalians cells, the general pattern of localization of the proteasome is a uniform repartition into the cytoplasm, with a slightly stronger labeling of the nucleus. However, it is interesting to note that in some degenerative disorders, the proteasome is relocalized into intracytoplasmic inclusions. Furthermore, upon proteasome inhibition or upon proteasome target overexpression, a perinuclear aggregate accumulates at the vicinity of the centrosome. This structure, named aggresome, contains proteasome subunits and ubiquitylated proteins (for reviews see Kopito, 2000; Wojcik and DeMartino, 2003). In contrast, yeast PSGs do not colocalize with spindle pole body (the yeast equivalent of mammalian centrosome; Fig. S3 C). Whether cytoplasmic structures containing proteasome could form in mammalian cells under nonpathological conditions remains an open question. In yeasts, PSGs formation is triggered by the entry into quiescence. Because yeast quiescence share many features with G0 mammalian cells, it would be of great interest to find out whether PSG-like structures are conserved from yeasts to mammals.

Materials and methods

Yeast strains and growth conditions

All the *S. cerevisiae* strains used in this study are isogenic to BY4742, BY4741, or BY4743 (available from Euroscarf). *S. pombe* strain expressing Pad1-GFP from the endogenous locus is a gift from J.P Javerzat (Centre

National de la Recherche Scientifique, Institut de Biochimie et Génétique Cellulaires, Université Victor Segalen Bordeaux 2, UMR5095 Bordeaux, France; Wilkinson et al., 1998). Plasmids p3394, p3348, p3330, and p3350 integrate RFP (tdimer 2(12); Campbell et al., 2002) at the 3′ end of the *SCL1*, *RPT6*, *SEM1*, and *PUP1* endogenous loci, respectively. Details of the constructions are available upon request. Yeast growing media are described in Sagot et al. (2006).

GFP fusion proteins

Yeast strains carrying GFP fusions used in this study were obtained from Invitrogen (gift from B. Goode, Rosenstiel Center, Brandeis University, Waltham, MA). The steady-state level of the 21 proteasome subunits fused to GFP studied remained unchanged throughout 7 d of culture (Fig. S1). This confirms the primary findings of Bajorek et al. (2003), which have shown that the level of the two 19S subunits Rpn3p and Rpn10p remained constant even after 9 d in stationary phase.

Microscopy

For live cell imaging, yeast cells were grown at 30°C in YPDA. 2–2.5 µl of the culture was spotted onto a glass slide and immediately imaged at room temperature. For refeeding experiments, cells were centrifuged and the supernatant, i.e., the "old" YPDA medium, was filtered to remove nonpelleted cells. Cells were then refed with prewarmed (30°C) "new" YPDA or old YPDA at an OD 600 nm of ∼0.6–0.8 and grown in Erlenmeyer flask in a 30°C water bath. For cycloheximide experiments, a 4-d-old culture was preincubated for 1 h with 100 µg/ml cycloheximide (Sigma-Aldrich). Cells were then pelleted and resuspended at an OD 600 nm of ∼0.6–0.8 in new YPDA medium containing 100 µg/ml cycloheximide. The protocol used for actin staining was described in Sagot et al. (2002).

For cell classification, when the proteasome signal was detected diffusely within the nucleus (Fig. 1 C, top, and D and F, left), cells were scored as "nuclear". When the proteasome signal was detected at the nuclear periphery with a clear absence of signal inside the nucleus, cells were scored as "nuclear periphery" if the fluorescence was even all around the nuclear periphery (Fig. 1 C, top middle, and D and E, middle left), and as "dot close to the nuclear periphery" as soon as more clearly intense immobile dot close to the nuclear membrane was detected (Fig. 1 C, middle bottom, and D and E, middle right). As soon as a bright dot was detectable moving inside the cytoplasm, cells were scored as "PSG" (Fig. 1 C, bottom, and D and E, right).

Cells were observed in a fully automated inverted microscope (200M; Carl Zeiss, Inc.) equipped with a MS-2000 stage (Applied Scientific Instrumentation), a xenon light source (Lambda LS 175 W; Sutter Instrument Co.), a 100× 1.4 NA Plan-Apochromat objective, and a five-position filter turret. For live cell GFP imaging, we used FITC (excitation, HQ487/25; emission, HQ535/40; beamsplitter, Q505lp). For GFP/RFP colocalization, we used FITC and Cy3 (excitation, HQ535/50; emission, HQ610/75; beamsplitter, Q565lp). Images were acquired using a camera (CoolSnap HQ; Roper Scientific). The microscope, camera, and shutters (Uniblitz) were controlled by SlideBook software (4.1; Intelligent Imaging Innovations). Images are, unless specified, maximal projection of z stacks performed using a 0.2-µm step. Intensity measurements were done on maximal projections of 0.2-µm step z stacks. The mean intensity of a 12-pixel region was measured using SlideBook and the background intensity was subtracted. Motility measurements were done on single focal plane time lapse (one image per second). Images were segmented according to the intensity. The center of intensity displacement between each focal plane was measured using the SlideBook particle tracking application.

Electron microscopy was done as described in Sagot et al. (2006) using yeast cells grown for 4 d in YPDA. Primary antibodies were polyclonal rabbit anti-20S proteasome diluted 1/250 (Novus Biologicals). Secondary antibodies were anti–rabbit IgG conjugated to 10-nm gold particles (BioCell Laboratories, Inc.). Specimens were observed with a 120-kV electron microscope (Tecnai 12 Biotwin; Philips) at the electron microscopy facility of the Service Commun de Microscopie, (Pôle de Microscopie Electronique de la Plateforme Génomique Fonctionnelle Bordeaux, Université Victor Ségalen Bordeaux 2).

Miscellaneous

Glucose concentration was measured using the D-Glucose/D-Fructose UV test kit (Roche).

Online supplemental material

Fig. S1 shows the steady-state level of different proteasome subunits fused to GFP detected by Western blot. Fig. S2 addresses the proteasome assembly status and activity in total cell extracts by native gel electrophoresis followed by incubation with LLVY-AMC in the presence of ATP and SDS. In Fig. S3, diagrams describing the intensity and mobility of PSGs are shown. Images of colocalization experiments between the proteasome and the spindle pole body are also provided. Table S1 shows the localization pattern of 21 out of the 33 proteasome 26S subunits. Online supplemental material is available at http://www.jcb.org/cgi/content/full/jcb.200711154/DC1.

We wish to thank Bruce Goode and Jean-Paul Javerzat for sharing reagents and Jean-Paul Javerzat and Benoît Pinson for helpful discussions and comments on the manuscript. We thank Marie-France Giraud for assistance with blue native PAGE.

This work was supported by a Young Investigator grant from the Agence Nationale pour la Recherche (JC05_42065 to I. Sagot) and a grant from l'Association pour la Recherche sur le Cancer (ARC#4855 to B. Daignan-Fornier). D. Laporte was supported by a Ministère de l'Education Nationale et de la Recherche doctoral fellowship. The microscope was financed by the Conseil Regional d'Aquitaine.

Submitted: 29 November 2007
Accepted: 1 May 2008

References

Bajorek, M., D. Finley, and M.H. Glickman. 2003. Proteasome disassembly and downregulation is correlated with viability during stationary phase. *Curr. Biol.* 13:1140–1144.

Campbell, R.E., O. Tour, A.E. Palmer, P.A. Steinbach, G.S. Baird, D.A. Zacharias, and R.Y. Tsien. 2002. A monomeric red fluorescent protein. *Proc. Natl. Acad. Sci. USA.* 99:7877–7882.

Collins, G.A., and W.P. Tansey. 2006. The proteasome: a utility tool for transcription? *Curr. Opin. Genet. Dev.* 16:197–202.

Enenkel, C., A. Lehmann, and P.M. Kloetzel. 1998. Subcellular distribution of proteasomes implicates a major location of protein degradation in the nuclear envelope-ER network in yeast. *EMBO J.* 17:6144–6154.

Fehlker, M., P. Wendler, A. Lehmann, and C. Enenkel. 2003. Blm3 is part of nascent proteasomes and is involved in a late stage of nuclear proteasome assembly. *EMBO Rep.* 4:959–963.

Ferdous, A., F. Gonzalez, L. Sun, T. Kodadek, and S.A. Johnston. 2001. The 19S regulatory particle of the proteasome is required for efficient transcription elongation by RNA polymerase II. *Mol. Cell.* 7:981–991.

Hanna, J., and D. Finley. 2007. A proteasome for all occasions. *FEBS Lett.* 581:2854–2861.

Heinemeyer, W., P.C. Ramos, and R.J. Dohmen. 2004. The ultimate nanoscale mincer: assembly, structure and active sites of the 20S proteasome core. *Cell. Mol. Life Sci.* 61:1562–1578.

Isono, E., K. Nishihara, Y. Saeki, H. Yashiroda, N. Kamata, L. Ge, T. Ueda, Y. Kikuchi, K. Tanaka, A. Nakano, and A. Toh-e. 2007. The assembly pathway of the 19S regulatory particle of the yeast 26S proteasome. *Mol. Biol. Cell.* 18:569–580.

Kopito, R.R. 2000. Aggresomes, inclusion bodies and protein aggregation. *Trends Cell Biol.* 10:524–530.

Lee, D.H., and A.L. Goldberg. 1996. Selective inhibitors of the proteasome-dependent and vacuolar pathways of protein degradation in *Saccharomyces cerevisiae*. *J. Biol. Chem.* 271:27280–27284.

Lehmann, A., K. Janek, B. Braun, P.M. Kloetzel, and C. Enenkel. 2002. 20 S proteasomes are imported as precursor complexes into the nucleus of yeast. *J. Mol. Biol.* 317:401–413.

Li, X., A.R. Kusmierczyk, P. Wong, A. Emili, and M. Hochstrasser. 2007. beta-Subunit appendages promote 20S proteasome assembly by overcoming an Ump1-dependent checkpoint. *EMBO J.* 26:2339–2349.

McDonald, H.B., and B. Byers. 1997. A proteasome cap subunit required for spindle pole body duplication in yeast. *J. Cell Biol.* 137:539–553.

Orlowski, M., and S. Wilk. 2003. Ubiquitin-independent proteolytic functions of the proteasome. *Arch. Biochem. Biophys.* 415:1–5.

Parker, R., and U. Sheth. 2007. P bodies and the control of mRNA translation and degradation. *Mol. Cell.* 25:635–646.

Russell, S.J., K.A. Steger, and S.A. Johnston. 1999. Subcellular localization, stoichiometry, and protein levels of 26 S proteasome subunits in yeast. *J. Biol. Chem.* 274:21943–21952.

Sagot, I., S.K. Klee, and D. Pellman. 2002. Yeast formins regulate cell polarity by controlling the assembly of actin cables. *Nat. Cell Biol.* 4:42–50.

Sagot, I., B. Pinson, B. Salin, and B. Daignan-Fornier. 2006. Actin bodies in yeast quiescent cells: an immediately available actin reserve? *Mol. Biol. Cell.* 17:4645–4655.

Schmidt, M., J. Hanna, S. Elsasser, and D. Finley. 2005. Proteasome-associated proteins: regulation of a proteolytic machine. *Biol. Chem.* 386:725–737.

Sulahian, R., D. Sikder, S.A. Johnston, and T. Kodadek. 2006. The proteasomal ATPase complex is required for stress-induced transcription in yeast. *Nucleic Acids Res.* 34:1351–1357.

Takeda, K., and M. Yanagida. 2005. Regulation of nuclear proteasome by Rhp6/Ubc2 through ubiquitination and destruction of the sensor and anchor Cut8. *Cell.* 122:393–405.

Tatebe, H., and M. Yanagida. 2000. Cut8, essential for anaphase, controls localization of 26S proteasome, facilitating destruction of cyclin and Cut2. *Curr. Biol.* 10:1329–1338.

Wendler, P., A. Lehmann, K. Janek, S. Baumgart, and C. Enenkel. 2004. The bipartite nuclear localization sequence of Rpn2 is required for nuclear import of proteasomal base complexes via karyopherin alphabeta and proteasome functions. *J. Biol. Chem.* 279:37751–37762.

Wilkinson, C.R., M. Wallace, M. Morphew, P. Perry, R. Allshire, J.P. Javerzat, J.R. McIntosh, and C. Gordon. 1998. Localization of the 26S proteasome during mitosis and meiosis in fission yeast. *EMBO J.* 17:6465–6476.

Wojcik, C., and G.N. DeMartino. 2003. Intracellular localization of proteasomes. *Int. J. Biochem. Cell Biol.* 35:579–589.